JOC Article
pubs.acs.org/joc

NXO Building Blocks for Backbone Modification of Peptides and Preparation of Pseudopeptides

Constantin Rabong, Ulrich Jordis,* and Jaywant B. Phopase*

Institute of Applied Synthetic Chemistry, Vienna University of Technology, Getreidemarkt 9, 1060 Vienna, Austria

jaywant.phopase@dcu.ie; ujordis@pop.tuwien.ac.at

Received November 26, 2009

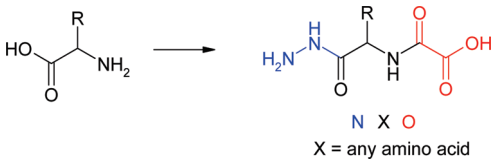

The design and synthesis of novel building blocks for peptide modification, termed "NXO", is reported. We describe the utility of these building blocks to prepare new pseudo- and oligopeptides and demonstrate the efficient assembly of modified tripeptides using both conventional liquid phase peptide synthesis and solid supported synthesis. Pertaining to the study of NXO in peptide mimicry, the structure of NXO-incorporating tripeptide β-strand mimics was investigated in the N^{L}AlaO incorporating β-sheet model compound **13**. Evidenced by spectroscopy and computation, **13** selectively adopts a β-structure in chloroform and characteristically samples the NXO-modified backbone site in the core β-sheet region. ROESY (HNMR) and molecular dynamics data suggest that when disrupting the cross-strand hydrogen-bonding pattern by switching the solvent from $CDCl_3$ to d_3-MeOH, the main conformation with peptide and NXO-peptide backbones similar to that in root mean square deviation of corresponding backbone atoms (rmsd) is preserved.

Introduction

Though naturally occurring and synthetic peptides are promising leads for drug discovery, their therapeutical application has been limited.[1] This arises from their rapid metabolism, poor bioavailability, and short duration of action. Many peptide analogues have been synthesized to date through the modification of not only the amino acid side chain, but also the backbone structure.[2,3] The general strategy involved in peptide backbone $(-NH-CHR-CO)_n$ modification is the change at any one of the repeating elements (NH, CHR, and CO) or a combined (CONH) unit of the peptide. Synthetically, modification at the α-carbon in the peptide backbone remains the most challenging task. Only a few examples of backbone modification at the α-carbon in peptides exist.[4] The most common manipulation involving the α-carbon atom of peptides is the inversion of stereochemistry to yield D-amino acids.[5] Azapeptides[2a,4a,d] and oxalo-retro

(1) (a) Ordero, F. M.; Salvati, M.; Vurchio, C.; de Mejeire, A.; Brandi, A. *J. Org. Chem.* **2009**, *74*, 4225−4231 and references cited therein. (b) Purcell, A. W.; McCluskey, J.; Rossjohn, J. *Nat. Rev. Drug Discovery* **2007**, *6*, 404–414. (c) Perez, J. J.; Corcho, F.; Llorens, O. *Curr. Med. Chem.* **2002**, *9*, 2209–2229. (d) Bursavich, M. G.; Rich, D. H. *J. Med. Chem.* **2002**, *45*, 541–558. (e) Dougherty, J. M.; Probst, D. A.; Robinson, R. E.; Moore, J. D.; Klein, T. A.; Snelgrove, K. A.; Hanson, P. R. *Tetrahedron* **2000**, *56*, 9781–9790. (f) Hruby, V. J.; Balse, P. M. *Curr. Med. Chem.* **2000**, *7*, 945–970. (g) Steer, D. L.; Lew, R. A.; Perlmutter, P.; Smith, A. I.; Aguilar, M.-I. *Curr. Med. Chem.* **2002**, *9*, 811–822.

(2) (a) Crepin, A.; Wattier, N.; Petit, S.; Bischoff, L.; Fruit, C.; Marsais, F. *Org. Biomol. Chem.* **2009**, *7*, 128–134. (b) Cardillo, G.; Gentilucci, L.; Tolomelli, A. *Mini Rev. Med. Chem.* **2006**, *6*, 293–304. (c) Melendez, R. E.; Lubell, W. D. *J. Am. Chem. Soc.* **2004**, *126*, 6759−6764 and references cited therein. (d) Marshall, G. R. *Tetrahedron* **1993**, *49*, 3547–3558. (e) Han, H.; Yoon, J.; Janda, K. D. *Methods Mol. Med.* **1999**, *23*, 87. (f) Perdih, A.; Sollner, D. M. *Curr. Org. Chem.* **2007**, *11*, 801–832. (g) Zhao, L.; Li, C.-J. *Angew. Chem., Int. Ed.* **2008**, *47*, 7075–7078.

(3) (a) Han, H.; Janda, K. D. *J. Am. Chem. Soc.* **1996**, *118*, 2539–2544. (b) Hagihara, M.; Anthony, N. J.; Stout, T. J.; Clardy, J.; Schreiber, S. J. *J. Am. Chem. Soc.* **1992**, *114*, 6568–6570. (c) Simon, R. J..; et al. *Proc. Natl. Acad. Sci. U.S.A.* **1992**, *89*, 9367–9371. (d) Smith, A. B.; Keenan, T. P.; Holcomb, R. C.; Sprengeler, P. A.; Guzman, M. C.; Wood, J. L.; Carroll, P. J.; Hirschmann, R. *J. Am. Chem. Soc.* **1992**, *114*, 10672–10674. (e) Cho, C. Y.; Moran, E. J.; Cherry, S. R.; Stephans, J. C.; Fodor, S. P.; Adams, C. L.; Sundaaram, A.; Jacobs, J. W.; Schultz, P. G. *Science* **1993**, *261*, 1303–1305. (f) Liskamp, R.-M. J. *Angew. Chem., Int. Ed. Engl.* **1994**, *33*, 633–636. (g) Burgess, K.; Linthicum, D. S.; Shin, H. *Angew. Chem., Int. Ed. Engl.* **1995**, *34*, 907–909.

(4) (a) Gante, J. *Synthesis* **1989**, 405–413. (b) Sherman, D. B.; Spatola, A. F. *J. Am. Chem. Soc.* **1990**, *112*, 433–441. (c) Hirschmann, R. *Angew. Chem., Int. Ed. Engl.* **1991**, *30*, 1278–1301. (d) Gante, J. *Angew. Chem., Int. Ed. Engl.* **1994**, *33*, 1699–1720.

(5) (a) Spatola, A. F. In *Chemistry and Biochemistry of Amino Acids, Peptides and Proteins*; Weinstein, B., Ed.; Marcel Dekker: New York, 1983; Vol. VII, 267−357. (b) Milton, R. C.; Milton, S. C.; Kent, S. B. *Science* **1992**, *256*, 1445–1448.

Published on Web 03/18/2010 DOI: 10.1021/jo902518r

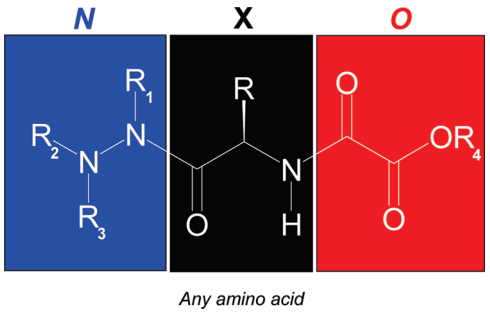

FIGURE 1. X = any amino acid, R^1-R^4 = H, alkyl, aryl, protecting group.

peptides[6] are further examples of α-carbon modification; although studies toward biologically active analogues of these have had significant success,[2a,6d] their synthetic exploitation remained underexplored.[2,4a,d,6]

In this article, we describe the design of novel building blocks and their use in peptide synthesis and as tripeptide β-strand mimics to prepare β-sheet-like compounds.

Results and Discussion

We envisioned modifying amino acids to give new kinds of pseudopeptides with reverse functionalities on either end by incorporating an oxalic acid functionality at the amine end and a hydrazine functionality at the carboxylic acid end. Thus, the amino group in the parent amino acid is converted to the oxalamide (and therefore becomes the C-terminus of the pseudopeptide) and the acid is converted to the azapeptide (thus being converted to the N-terminus); however, the amino acid core of the parent amino acid remains unchanged (Figure 1). We designated this new class of pseudopeptides by a three-letter abbreviation as "NXO", where "N" represents the hydrazide part, "O" represents the oxalamide part, and "X" is the three-letter abbreviation of the parent amino acid (see Table 1).

NXO constitutes a short-range, dipole-organized motif. Its "N-" and "O"-retrons have an inherent bias toward antiparallel dipole configuration.[7] By incorporating such features into an NXO-modified backbone, they should lend themselves naturally to β-structure mimicry. It is instructive to note that NXO-modified peptides are β-sheet-tripeptide mimics that comprise the oxalo-retro modification and azapeptide modification on either ends. While doing so, the α-carbon atoms of the amino acids at both ends of the tripeptide are converted from sp^3-hybridized, chiral centers to sp^2 centers that impose additional rigidity and extended conjugation to the peptide strand (Figure 2).

Any advanced scaffold must aim to meet the requirements of a peptidomimetic in terms of being a "peptide foldamer":[8] diversifiable, highly designable, efficiently prepared, and selectively adopting an *in silico* predictable secondary structure. NXO, its features endowed within each monomer, unites the "*beta-oid*" template with the strand increment at the repeating unit level. Featuring the backbone polarization pattern of α-amino acids (Figure 2), it is amenable for use in mixed peptides and as a biopolymer in its own right.

Synthesis of Orthogonally Protected NXO Building Blocks. Our first goal was to prepare orthogonally protected NXO building blocks **3** starting from different amino acids that can be incorporated into peptide synthesis from either the C- or N-terminal after selective deprotection. As numerous Boc, Fmoc, Z-protected substituted hydrazines,[9] as well as a variety of different oxalic acid diesters **2**, are synthetically available,[10] a large variety of orthogonally protected NXO building blocks can be prepared.

We developed a robust one-pot methodology to prepare NXO building blocks starting from commercially available amino acids (Scheme 1). The amino acid **1** is reacted with the appropriate oxalic acid diester **2**, prepared in near-quantitative yields by reacting corresponding alkyl oxalyl chlorides with 4-nitrophenol in pyridine-CH_2Cl_2, in DMF at 50 °C for 1.5 h. Further treatment of the resulting reaction mixture with an appropriately protected hydrazine at room temperature affords the desired NXO building blocks. The advantage of this method is that the amino acids do not require any protection at the amino group, thus decreasing the number of synthetic steps.[11] This method allowed for the efficient preparation of the building blocks presented in Table 1 in good to excellent yields. The chiral purity of compounds **3c** and **3f** was analyzed by HPLC, using a Chiral Technologies Chiral Cel OD-H column, eluting with 90% *n*-heptane/0.1% diethylamine/9.9% isopropanol as mobile phase. The minimum detection limit of the other enantiomer was established to be $<0.04\%$; therefore, the chiral purity of the NXO building blocks exceeded 99.96% in both cases.

(6) (a) Ranganathan, D.; Saini, S. *J. Am. Chem. Soc.* **1991**, *113*, 1042–1044. (b) Ranganathan, D. *Pure Appl. Chem.* **1996**, *68*, 671–674. (c) Ranganathan, D.; Vaish, N. K.; Shah, K. *J. Am. Chem. Soc.* **1994**, *116*, 6545–6557. (d) Murahashi, S-I.; Mitani, A.; Kitao, K. *Tetrahedron* **2000**, *41*, 10245−1049 and references cited therein.

(7) (a) Guenther, R.; Hofmann, H.-J. *J. Am. Chem. Soc.* **2001**, *123*, 247–255. (b) Thormann, M.; Hofmann, H.-J. *THEOCHEM* **1999**, *469*, 63−76 and references cited therein; see also refs 4d and 6b. These references contain several important points which guided our design considerations employing substituted hydrazines and oxalates (at the peptidic C- and N-ends, respectively) to replace amides as well as stereogenic α-amino-carbons in the peptide backbone: Introduced nitrogens were shown to be substantially pyramidal and hence potentially stereogenic (ref 7a) and to engage heavily in hydrogen bonding to neighboring carbonyl oxygen (C5 interactions and also, to a lesser extent, C8 interactions). In general, azapeptides were considered to be a poor choice when extended strand mimics are sought after and described as intrinsically biased for helix/turn formation (ref 7b; see also 8b). However, they possess a high propensity for turn mimicry as they sample all known β-turn types within the configuration space also adopted by amino acids. Aza-amino acids at the i + 2 position favor a type II turn, whereas at the i + 1 site, a type I turn is preferred. On the other hand, dicarbonylhydrazides were shown to have a propensity for an N−N bond orientation with perpendicular lone pairs (ref 7a) but there is also experimental evidence that when a dicarbonyl-substituted aza-linkage is allowed to engage in hydrogen bonding, planarity can be enforced. Ab initio methods employing correlation-polarization basis sets with explicitly treated aqueous solvation on formylated azaglycine gave the relevant backbone dihedrals exclusively in the core β and α region ($\Phi \approx (-70)°$ and $(-90)°$ and $\psi \approx +165°$ and $(-25)°$ for β and α, respectively). Moreover, stereogenicity was highly pronounced in the β region but an overtly planarized nitrogen is observed in the α region. Most importantly, the authors concluded that side chains on the azapeptide nitrogens had almost no influence on the backbone torsion profile established before. Studies on oxalo-retro bispeptides (see refs 6a−c) had shown that a peptide-isosteric MeO_2C-Leu-$HNCO_2CNH$-Leu-CO_2Me unit is mainly in a bicyclo[3.3.0] motif, that is, extensive next-neighbor hydrogen bonding occurs, imposing strong planarizing bias toward an extended conformation.

(8) (a) Gellman, S. H. *Acc. Chem. Res.* **1998**, *31*, 173–180. (b) Hill, D. J.; Mio, M. J.; Prince, R. B.; Hughes, T. S.; Moore, J. S. *Chem. Rev.* **2001**, *101*, 3893–4012.

(9) (a) Dutta, A. S.; Morley, J. S. *J. Chem. Soc., Perkin Trans. 1* **1975**, 712–1720. (b) Quibell, M.; Turnell, W. G.; Johnson, T. *J. Chem. Soc., Perkin Trans. 1* **1993**, 2843–2849. (c) Bentley, P. H.; Morley, J. S. *J. Chem. Soc., Perkin Trans. 1* **1966**, 60–64. (d) Biel, J. H.; Drukker, A. E.; Mitchell, T. F.; Sprengeler, E. P.; Nuhfer, P. A.; Conway, A. C.; Horita, A. *J. Am. Chem. Soc.* **1959**, *81*, 2805–2813. (e) Rutjes, F.-P. J. T.; Teerhuis, N. M.; Hiemstra, H.; Speckkamp, W. N. *Tetrahedron* **1993**, *49*, 8605–8628.

(10) (a) Vashchenko, Y. N.; Moshchitskii, S. D.; Kirsanov, A. V. *Zh. Obshch. Khim.* **1962**, *32*, 3765–3768. (b) Chakraborty, K.; Devakumar, C. *J. Agric. Food Chem.* **2006**, *54*, 1868–1873.

(11) Some of these building blocks have been prepared by us in a more classical manner before, see: PCT Int. Appl. **2007**, WO2007095980.

TABLE 1. Orthogonally Protected NXO Building Blocks

entry	R^2	R^4	R^3, R^1	X	NXO-name	$[\alpha]^{20}_D$ (*c* 0.5, CH_3OH)	isolated yield (%)
1	Boc	Me	H, H	Phe	Boc-NPheO-OMe (**3a**)	−28.6	92
2	Fmoc	Me	H, H	Phe	Fmoc-NPheO-OMe (**3b**)	−19.4	61
3	Fmoc	Bu^t	H, H	Phe	Fmoc-NPheO-OBu^t (**3c**)	−18.0[a]	94
4	Fmoc	Bu^t	H, Me	Phe	Fmoc-N(Me)PheO-OBu^t (**3d**)	+26.4	83
5	Fmoc	Bu^t	Me, H	Phe	Fmoc-(Me)NPheO-OBu^t (**3e**)	−17.4	87
6	Cbz	Bu^t	H, H	Phe	Cbz-NPheO-OBu^t (**3f**)	−23.0	89
7	Cbz	Me	H, H	Phe	Cbz-NPheO-OMe (**3g**)	24.6	94
8	Fmoc	Me	H, H	Trp	Fmoc-NTrpO-OMe (**3h**)	−37.2	85
9	Fmoc	Bu^t	H, H	Trp	Fmoc-NTrpO-OBu^t (**3i**)	−37.2	83
10	Cbz	Me	H, H	Trp	Cbz-NTrpO-OMe (**3j**)	−37.4	78
11	Fmoc	Me	H, H	Tyr(2Br-Z)OH	Fmoc-NTyr (2Br-Z) O-OMe (**3k**)	−10.2[a]	88
12	Fmoc	Bu^t	H, H	Tyr(2Br-Z)OH	Fmoc-NTyr (2Br-Z) O-OBu^t (**3l**)	−12.4	84
13	Cbz	Bu^t	H, H	Tyr(2Br-Z)OH	Cbz-NTyr (2Br-Z) O-OBu^t (**3m**)	−10.4	94
14	Cbz	Me	H, H	Tyr(2Br-Z)OH	Cbz-NTyr (2Br-Z) O-OMe (**3n**)	−9.0	94
15	Boc	Me	H, H	Leu	Boc-NLeuO-OMe (**3o**)	−43.4	75
16	Fmoc	Bu^t	H, H	Leu	Fmoc-NLeuO-OBu^t (**3p**)	−35.2	88
17	Cbz	Me	H, H	Leu	Fmoc-NLeuO-OMe (**3q**)	−43.8	88
18	Fmoc	Bu^t	H, H	Pro	Fmoc-NProO-OBu^t (**3r**)	−68.6	98
19	Cbz	Bu^t	H, H	Pro	Cbz-NProO-OBu^t (**3s**)	−70.8	99
20	Fmoc	Bu^t	H, H	Ala	Fmoc-NAlaO-OBu^t (**3t**)	−31.4	93
21	Cbz	Me	H, H	Ala	Cbz-NAlaO-OMe (**3u**)	−47.6	97
22	Fmoc	Bu^t	H, H	Ser(Bn)-OH	Fmoc-NSer(Bn)O-OBu^t (**3v**)	−6.2	81
23	Fmoc	Bu^t	H, H	Glu(OBn)OH	Fmoc-NGlu(OBn)O-OBu^t **3w**)	−22.8	78
24	Fmoc	Bu^t	H, H	Thr(Bn)OH	Fmoc-NThr(Bn)O-OBu^t (**3x**)	−8.0	67
25	Fmoc	Bu^t	H, H	Val	Fmoc-NValO-OBu^t (**3y**)	−31.6	82

[a]Optical rotation was measured in DMF.

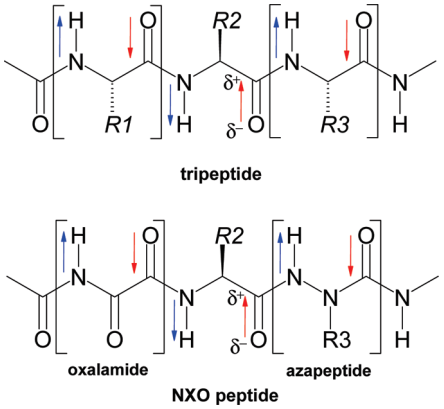

FIGURE 2. The donor−acceptor pattern of a tripeptide vs NXO peptide.

Synthesis of Pseudopeptides 4 and 5. In an effort to demonstrate the applicability of NXO building blocks, we utilized them to prepare pseudopeptides via liquid (**4**, Scheme 2) and solid phase (**5**, Scheme 3) protocols. Both pseudopeptides **4** and **5** were chosen as model peptides in order to demonstrate the ease of integrating the NXO building blocks in the synthesis of oligopeptides by using routine chemical manipulations. Pseudopeptide **4** was prepared from Boc-NPheO-OMe (**3a**) (Scheme 2).

The Boc protective group was removed by treatment with TFA−CH_2Cl_2 (1:1), and the free amine was liberated by treatment with triethylamine (TEA). The amino group was then coupled to Boc-L-alanine with DCC/HOBt to give **6**. The methyl ester was hydrolyzed by using LiOH in methanol to afford acid **7**, which after coupling to **8** with EDCI/HOBt affords compound **4** (73% overall yield).

Scheme 3 illustrates the solid phase synthesis of pseudopeptide **5**. Resin bound NXO peptide **10** was constructed on hydroxymethyl polystyrene resin by standard solid phase synthesis methods. The Boc protective group was removed by treatment with TFA−CH_2Cl_2 (1:1) and the free amino group was then liberated by treatment with diisopropylethylamine (DIPEA). The resulting amine was coupled to Boc-L-Ala with DIC, HOBt to give **11**. The Boc group of **11** was removed and the liberated amine was coupled to Boc-L-phenylalanine by employing similar reaction conditions as above. Finally, peptide **5** was isolated as the sodium salt from the resin by hydrolysis with sodium methoxide. The sodium salt was neutralized with 1 N HCl and the structure of pseudopeptide **5** (43% overall yield with respect to the resin loading) was verified with MALDI-TOF.

Preparation of an NXO-Tripeptide *β*-Strand Mimic. The NXO-modified peptide backbone can adopt extended conformations as in a tripeptide *β*-strand by virtue of the conformational restraints and extended conjugation imposed by NXO's azapeptide "N" and oxalo-retro peptide "O"-motifs. Thus, we anticipated that, by exchanging both termini of a given amino acid to an oxalamide and azapeptide, respectively, sufficient strand planarization bias[12] could be introduced to maintain a strand-extended alignment capable of multiple intramolecular hydrogen bonding.

To evaluate the structural properties of NXO acting as a tripeptide *β*-strand mimic, we implemented an NXO derivative to prepare the *β*-sheet model compound **13** (see Scheme 4). **13** was designed by using a proven model system reported by Nowick and co-workers that consists of an oligourea molecular scaffold, *β*-strand mimic, and peptide strand.[13] There, it

(12) Archer, E. A.; Gong, H.; Krische, M. J. *Tetrahedron* **2001**, *57*, 1139–1159.

(13) (a) Nowick, J. S.; Tsai, J. H.; Bui, Q.-C. D.; Maitra, S. *J. Am. Chem. Soc.* **1999**, *121*, 8409–8410. (b) Nowick, J. S. *Acc. Chem. Res.* **1999**, *32*, 287–296. (c) Nowick, J. S.; Lam, K. S.; Khasanova, T. V.; Kemnitzer, W. E.; Maitra, S.; Mee, H. T.; Liu, R. *J. Am. Chem. Soc.* **2000**, *124*, 4972–4973. (d) Nowick, J. S.; Chung, D. M.; Maitra, K.; Maitra, S.; Stigers, K. D.; Sun, Y. *J. Am. Chem. Soc.* **2000**, *122*, 7654–7661. (e) Nowick, J. S. *Org. Biomol. Chem.* **2006**, *4*, 3869–3885. (f) Stigers, K. D.; Sun, Y. *J. Am. Chem. Soc.* **2000**, *122*, 7654–7661. (g) Nowick, J. S. *Org. Biomol. Chem.* **2006**, *4*, 3869–3885.

SCHEME 1. One-Pot Protocol To Prepare Orthogonally Protected NXO Building Blocks from α-Amino Acids

SCHEME 2. Solution-Phase Synthesis of Pseudopeptide 4

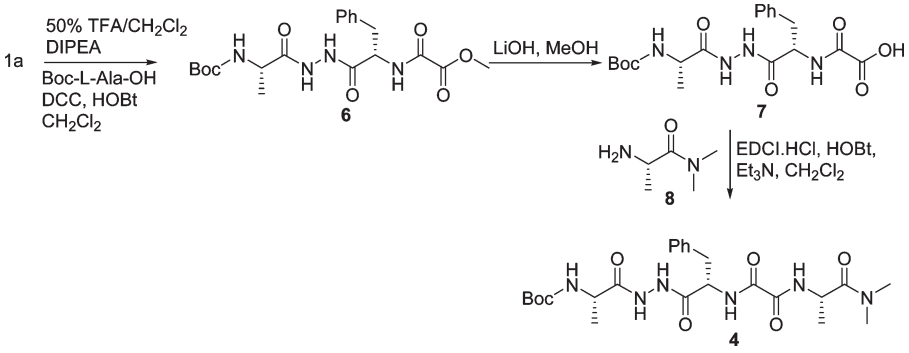

SCHEME 3. Solid-Phase Synthesis of Pseudopeptide 5

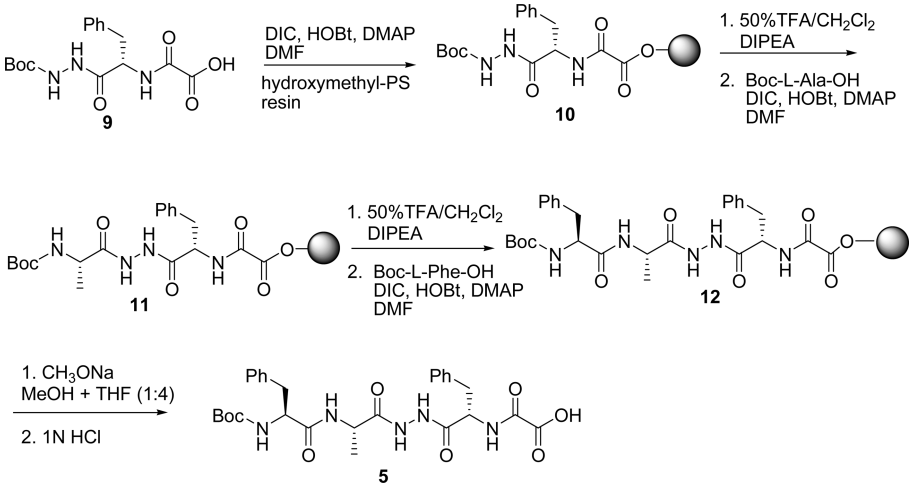

was shown that "hybrid" mimics where natural amino acids, in conjunction with conformationally restricted aromatic assembly templates, can selectively adopt well-defined secondary structure motifs.[14] Therefore, we aimed to test the foldability of an NXO-modified β-strand mimic in an oligo-urea turn unit (termed "molecular scaffold"[13]) in the context of what Nowick and co-workers have described as an "artificial β-sheet."[15]

To assess the performance of NXO in sheet-mimicry, we evaluated the same sequence of amino acids (Phe-Ile-Leu-NHMe) at corresponding[16] backbone positions. Knowing that Ala displays a rather insignificant intrinsic β-sheet propensity[17] we have, hence, incorporated an N^{L}AlaO unit into the lower strand section.

The synthesis of β-sheet-mimic **13** started from diamine **14**. Compound **14** was converted into urea **15** by reaction with phosgene to generate a carbamyl chloride group at the aniline nitrogen, followed by reaction with Boc-carbazate in dichloromethane. Subsequent deprotection of the Boc-protected hydrazide with TFA−CH_2Cl_2 (1:1) followed by liberation of the free amino group by treatment with DIPEA gave the amine that afforded, after coupling with compound **18**, compound **16** in 90% yield. Deprotection of Fmoc with 10% piperidine in DMF and further reacting the reaction mixture with acrylonitrile gave compound **17** in 50% yield. Compound **17** was converted into NXO-modified artificial β-sheet **13** by reaction with isocyanate **19**. Purification of the crude residue by column chromatography afforded 68% of **13**.

Conformation Analysis of 13. Part 1: ROESY NMR Studies. Extensive attempts to obtain single crystals of **13** suitable for X-ray diffraction analysis (XRD) have failed to date. Thus, secondary structure was investigated by solution NMR. Analysis of **13** in $CDCl_3$ at 290 K with 250 ms mixing

(14) Nowick, J. S. *Acc. Chem. Res.* **2008**, *41*, 1319−1330 and references cited therein.
(15) Nowick, J. S.; Smith, E. M.; Noronha, G. *J. Org. Chem.* **1995**, *60*, 7386–7387.
(16) (a) Nowick, J. S.; Holmes, D. L.; Mackin, G.; Noronha, G. A.; Shaka, J.; Smith, E. M. *J. Am. Chem. Soc.* **1996**, *118*, 2764–2765. (b) Nowick, J. S.; Pairish, M.; Lee, I. Q.; Holmes, D.; Ziller, J. W. *J. Am. Chem. Soc.* **1997**, *119*, 5413–5424.
(17) (a) Smith, C. K.; Withka, J. M.; Regan, L. *Biochemistry* **1994**, *33*, 5510–5517. (b) Smith, C. K.; Regan, L. *Acc. Chem. Res.* **1997**, *30*, 153–161. (c) Merkel, J. S.; Sturtevant, J. M.; Regan, L. *Structure* **1999**, *7*, 1333–1343. (d) Hughes, R. M.; Waters, M. L. *Curr. Op. Struct. Biol.* **2006**, *16*, 514–524.

SCHEME 4. Synthesis of NXO-Incorporating β-Sheet Mimic 13

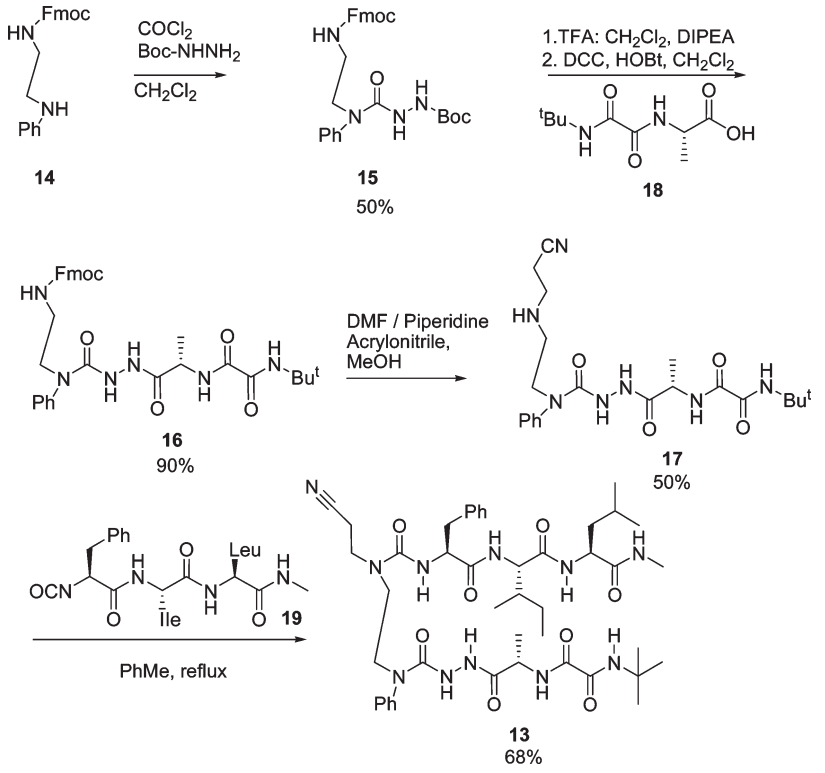

time at a concentration of 5 mM suggests population of the sample with a major conformer amounting to ≥94.8% based on averaged signal integration of H1, N−H28, and N−H32. The most compelling among the data are the NOEs between the lower strand substituent methyl and the phenylalanine benzyl-CH_2, H31↔H16, and between the upper strand isoleucine side chain and the α-amino proton, H30↔H10 and H30↔H12 (Figure 3; see also the Supporting Information). The across-strand NOE between the *tert*-butyloxalamido group and the terminal methylamide, H34↔H1, provides further strong evidence for the observed conformation to be in an intramolecularly strand-paired arrangement.[18] The presence of a weak NOE between the alanine methyl group and the terminal methylamide, H31↔H1, seems to reflect a curvature previously observed in *β*-sheet models at the C-end section.[19] Further, the vicinal coupling constant of the "X"-α-amino-proton with its neighboring amide-NH, $^3J_{H30\leftrightarrow HN32}$, was found to be 8.5 Hz.

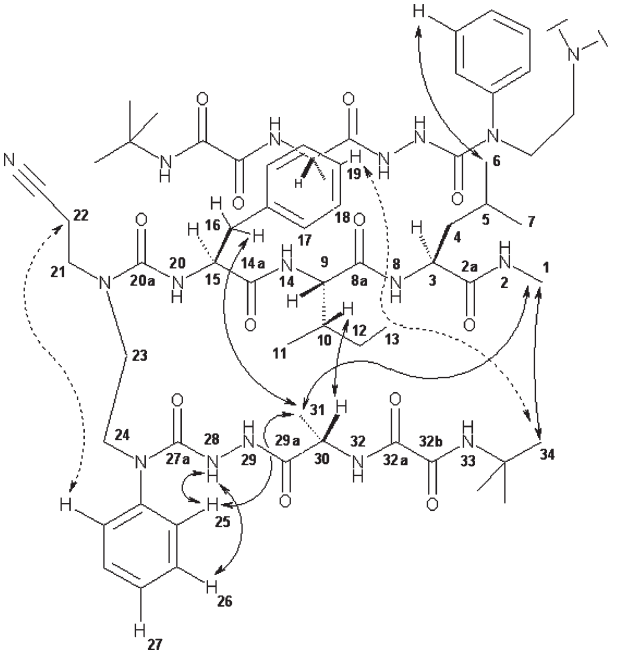

FIGURE 3. ROESY interactions in **13**. Spectra were recorded with a 250 ms mixing time at 290 K in $CDCl_3$ and d_3-MeOH. Full and dotted arrows represent the observed conformational key NOE enhancements in $CDCl_3$ and d_3-MeOH, respectively. Numbering is as used throughout the text. Notice that an intermolecular interaction is shown at the top of the figure; see also ref 19.

ROESY in d_3-MeOH exhibited some markedly different crosspeaks. Again, the spectra showed almost exclusively a single signal set to be populated in solution with the minor set amounting to <4.7% by averaged signal integration.

(18) (a) Nowick, J. S.; Smith, E. M.; Ziller, J. W.; Shaka, A. J. *Tetrahedron* **2002**, *58*, 727–739. (b) Chung, D. M.; Dou, Y.; Baldi, P.; Nowick, J. S. *J. Am. Chem. Soc.* **2005**, *127*, 9998–9999. see also ref 13d.

(19) Several NOEs account for *o*- and *m*-aniline-protons H25 and H26 to be close to the strand section C30−C28, suggesting the phenyl ring to be orthogonal to the lower strand amide backbone. H26 showed a medium NOE to the leucine-region C6−C7 multiplet, consistent with the previously invoked antiparallel edge-to-edge dimer formation in artificial *β*-sheet mimics, where a strand of one molecule binds the other strand of a second molecule in a 180° rotated fashion. (Nowick, J. S. *Org. Biomol. Chem.* **2006**, *4*, 3869−3885. On dimeric aggregation in particular: Nowick, J. S., Tsai, J. H.; Bui, Q.-C. D.; Maitra, S. *J. Am. Chem. Soc.* **1999**, *121*, 8409−8410. On self aggregation in *β*-sheets: Osterman, D. G.; Kaiser, E. T. *J. Cell. Biochem.* **1985**, *29*, 57−72.). By contrast, the minor conformation gave rise to a strong NOE H16↔H14 which was weak in the main conformer; H29↔H30 was seen but no H29↔H31. Moreover, a strong crosspeak H21↔H5/H4 in the minor conformer infers an alternative dimer pattern formation—homodimer or same-strand aggregation—to be present here (Nowick, J. S. *Org. Biomol. Chem.* **2006**, *4*, 3869−3885 and references cited therein).

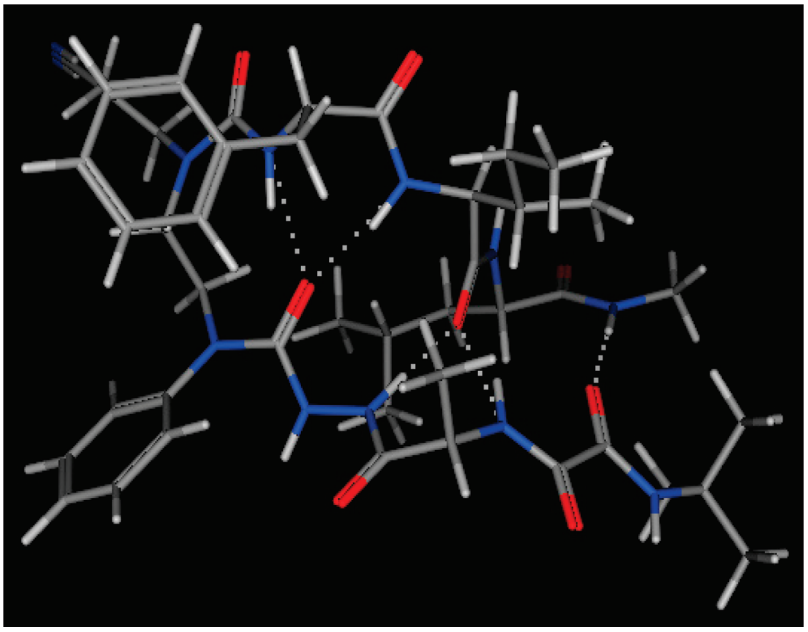

FIGURE 4. The minimum-energy conformer of **13** generated from stochastic searching with OPLS-AA parameters and also the central motif in rmsd-space during a 100 ns, 290 K MD simulation (see also the Supporting Information). Dotted lines indicate hydrogen bonding.

Weak-to-medium NOEs of the aniline-protons with the cyanoethylene side chain protons H22 and a prominent medium-to-strong NOE between the phenylalanine para-proton and the *tert*-butyloxalamide, H19↔H34, suggested a conformation with an alternating turn region to be present. Moreover, the crosspeaks H9↔H10, H10↔H14, and H31↔H32 were weaker in comparison to spectra recorded in $CDCl_3$ and there was a previously unobserved very weak interaction H3↔H11/H13.

In particular, TOCSY in d_3-MeOH gave insight into the hydrogen bonding behavior of the, now well-resolved, N−H signals (except for the N-hydrazide protons, N−H28 and 29, which exchanged under these conditions). All amide N−H signals were shifted downfield, some up to 1.2 ppm relative to measurements in $CDCl_3$, indicating strong augmentation of backbone hydrogen bonding in the more polar solvent (see Table 2, Supporting Information).

Conformation Analysis of 13. Part 2: Computational Analysis. Locating the Ensemble Minimum. To verify and substantiate the picture derived from NMR analysis, we performed exhaustive ($>10^5$ conformations generated) stochastic conformational searching around a loosely constrained, OPLS-AA[20]-derived input geometry satisfying the above-mentioned (see Figure 3 and the Supporting Information) conformationally diagnostic NOE requirements. An extended structure (Figure 4), across-strand associated via two "chelating" hydrogen bonds was detected as the energy-lowest conformer by 0.8 kcal.[21] This conformer was then freed of all restraints and subjected to molecular dynamics (MD), using the OPLS-AA parameter set and GB/SA[22] as an implicit solvation model.

Molecular Dynamics Trajectory Analyses, $CDCl_3$. At 290 and 300 K in $CDCl_3$, **13** presents a trajectory of strand−strand paired, extended sheet-like conformations within the sampled time span of 100 ns. The turn diaminoethane unit remains in an arrangement displaying N−C23−C24−N antiperiplanar (*ap*) during the entire simulation. At these temperatures, the hydrazide and in particular the oxalamide modifications are favored in a narrow torsional region (*ap*) +160° and −160°, respectively (see the Supporting Information).

Several indicative upper-to-lower strand hydrogen bonding interactions are present, notably O27a←HN20 (sampled 94% of the simulation time with an average lifetime of 31.5 ps), O29a←H28 (52.5%, 2.6 ps), O8a←H29 (22.2%, 7.5 ps), O8a←H32 (19.2%, 9 ps), O14a←H29 (14.8%, 2 ps), and O8a←H33 (12.7%, 2.8 ps). Moreover, from 600 MHz ^{1}H NMR in $CDCl_3$, we had observed $^3J_{H30↔HN32}$ to give a value of 8.5 Hz.[23] Since the dihedral corresponding to this torsion was adequately reproduced in the MD simulation (the dihedral displaying a maximum at −148° and thus satisfying the unparameterized Karplus equation[24]) we can, therefore, assess Φ (C32a−N32−C30−C29a) and Ψ (N32−C30−C29a−N29) in the N^LAlaO-modified strand. Φ and Ψ display maxima at −82° and +79°, respectively, thus sampling N^LAlaO in the core β-sheet-region of the Ramachandran plot.[25,26]

(20) Jorgensen, W. L.; Maxwell, D. S.; Tirado-Rives, J. *J. Am. Chem. Soc.* **1996**, *117*, 11225–11236.

(21) for instructive overviews on hydrogen bonding see: Schneider, H.-J. *Angew. Chem., Int. Ed.* **2009**, *48*, 3924–3977. Steiner, T. *Angew. Chem., Int. Ed.* **2002**, *41*, 48–76.

(22) Wojciechowski, M.; Lesyng, B. *J. Phys. Chem. B* **2004**, *108*, 18368–18376.

(23) (a) Wishart, D. S.; Sykes, B. D.; Richards, F. M. *Biochemistry* **1992**, *31*, 1647–1651. (b) Yu, H.; Daura, X.; van Gunsteren, W. F. *Proteins* **2004**, *54*, 116−127; see also: (c) Daura, X. *Theor. Chem. Acc.* **2006**, *116*, 297−306 and references cited therein. (d) Santivieri, C. M.; Jimenez, M. A.; Rico, M.; van Gunsteren, W. F.; Daura, X. *J. Peptide Sci.* **2004**, *10*, 546–565.

(24) (a) Karplus, M.; Anderson, D. H. *J. Chem. Phys.* **1959**, *30*, 6–10. (b) Karplus, M. *J. Chem. Phys.* **1959**, *30*, 11–15. (c) Karplus, M. *J. Am. Chem. Soc.* **1963**, *85*, 2870–2871.

(25) Ramachandran, G. N.; Ramakrishnan, C.; Sasisekharan, V. *J. Mol. Biol.* **1963**, *7*, 95–99.

(26) While the N^LAlaO Φ, ψ torsions in **13** appear to be at the lower end for what is expected for the central residue of a β-strand (Avbelj, F.; Moult, J. *Biochemistry* **1995**, *34*, 755−764.), there is evidence that many Ala-based proteins exhibit a maximum of Φ that is shifted around −90°. Φ around −80° was a minimum configuration as computed by ab initio methods in a two-stranded Ala dipeptide model (Shamovsky, I. L.; Ross, G. M.; Riopelle, R. J. *J Phys. Chem. B* **2000**, *104*, 11296−11307 and references cited therein; see also: Smith, L. J.; Bolin, K. A.; Schwalbe, H.; MacArthur, M. W.; Thornton, J. A.; Dobson, C. M.; *J. Mol. Biol.* **1996**, *255*, 494−506).

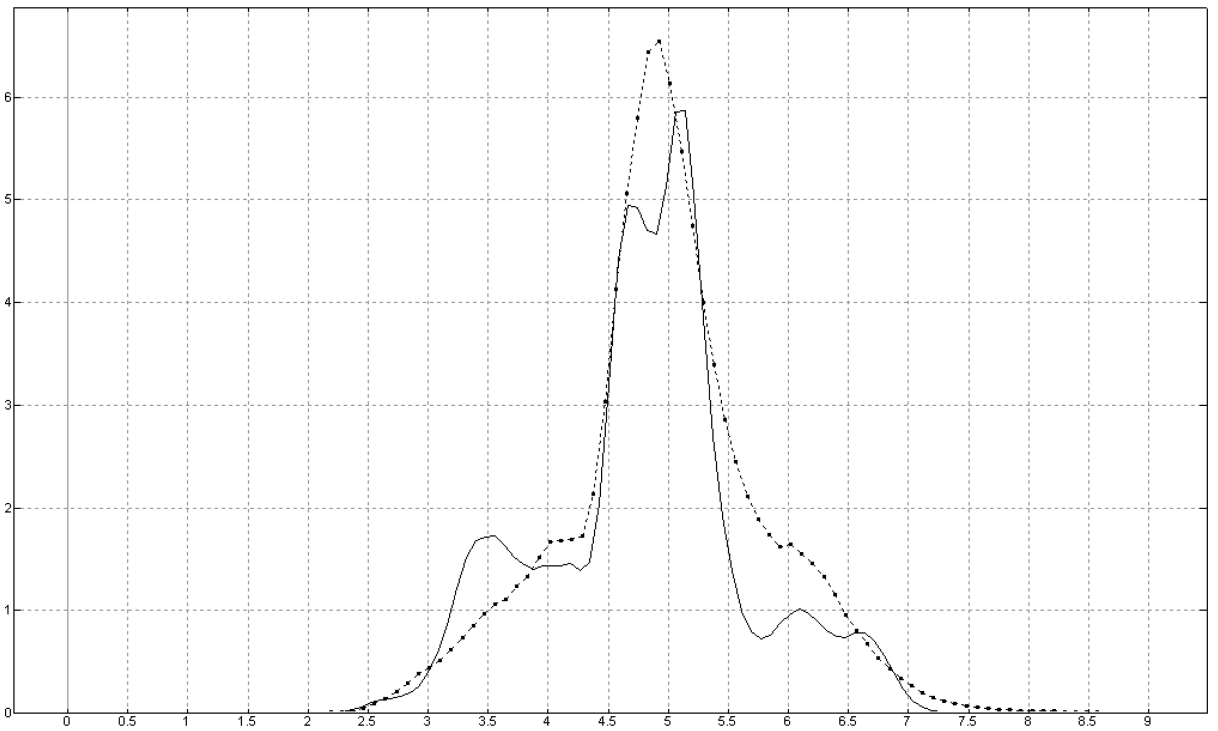

FIGURE 5. 13, Percentage-weighted rmsd[Å]-histogram of the 100 ns MD runs at 290 K. Solid and dotted lines indicate $CDCl_3$ ($\varepsilon = 4.8$) and MeOH ($\varepsilon = 32.5$) trajectories, respectively; RMSDs sampled at ≤25% atom, 50% atom, and 75% atom: 4.37, 4.87, 5.23 and 4.55, 4.95, 5.42 for $CDCl_3$ and MeOH, respectively.

Molecular Dynamics Trajectory Analyses, MeOH. It has been recognized that shielding of the peptide backbone dipoles by polar solvent molecules is a major contributor to solvation free energy. This in turn has a decisive influence on backbone conformation in proteins.[27] Upon switching from an aprotic, nonpolar solvent to one of relatively higher dielectric permittivity that is capable of hydrogen bonding, the polar solvent will compete with the solute for hydrogen-bonding interactions and introduce an increased desolvation free-energy penalty at the polar backbone. Then, as often the decisive influence that stabilizes the folded conformations is intrastrand hydrogen bonding,[28] the ensemble of conformational states in the solute−solvent system will experience a reorganization.

With β-sheet mimic **13** in MeOH, fewer stabilizing strand−strand hydrogen bonds were observed compared to $CDCl_3$. The diaminoethane turn-linker, displayed exclusively (*ap*) in $CDCl_3$, is sampled partially (*sc*) similar to prior observation in competitive solvents.[29] In this configuration, the linker can place the backbone carbonyl dipoles in an orientation with increased probability for favorable hydrophilic interaction,[27b] the pronounced increase in backbone solvation being mirrored in the observed downfield shifting of corresponding amino protons (see Table 2, Supporting Information). Strikingly, the lack in cross-strand hydrogen bonding interactions is unreflected in the backbone rmsd (Figures 5 and 6) that is still centered around rmsd 4.9, in the same region as the two ensemble maxima in the $CDCl_3$ simulation. In the ROESY experiments, measurements in both solvents showed a single but different major conformation. The observed H22↔H25 and H19↔H34 interactions are well-reproduced by molecular dynamics and subset analysis explains why no NOE across the strand-ends was observed in the more polar solvent: In MeOH, the NXO-mimic is still vastly sampled in a folded conformation with both strands extended and aligned, however, with relatively diminished across-strand hydrogen bonding. An increase in rotational flexibility, in particular the pronounced fraying of strand ends and less well-defined side chain rotamer preferences in the more polar solvent, is mirrored in overall decreased subset lifetimes (see Figure 5 and rmsd histograms in Figures 5 and 6 in the Supporting Information). Also, a minor fraction of conformation space represents the unfolded molecule.

Conclusion

Oligopeptides usually display a highly dynamic solution behavior, populating multiple low-energy conformations.[30] When one sets about a task related to this field of research, the structural plurality has to be defined. It is known that β-sheets in proteins exhibit potential energy surfaces with multiple energy-minima.[31] Yet, biological action is exerted via chemical entities appended to the secondary structure element; the arising tertiary structure then plays the decisive role in directing molecular recognition, e.g., receptor−ligand

(27) (a) Avbelj, F. *J. Mol. Biol.* **2000**, *300*, 1335–1359. (b) Baldwin, R. L. *J. Mol. Biol.* **2007**, *371*, 283−301 and references cited therein.

(28) Prabhu, N.; Sharp, K. *Chem. Rev.* **2006**, *106*, 1616−1623 and references cited therein.

(29) Junquera, E.; Nowick, J. S. *J. Org. Chem.* **1999**, *64*, 2527–2531. See also ref 22.

(30) Dill, K. A. *Biochemistry* **1990**, *29*, 7133−55; see also ref 27b.

(31) (a) Lacroix, E.; Kortemme, T.; Lopez de la Paz, M.; Serrano, L. *Curr. Op. Struct. Biol.* **1999**, *9*, 487−493 and references cited therein. (b) Street, A. G.; Mayo, S. L. AS **1999**, *96*, 9074−9076.

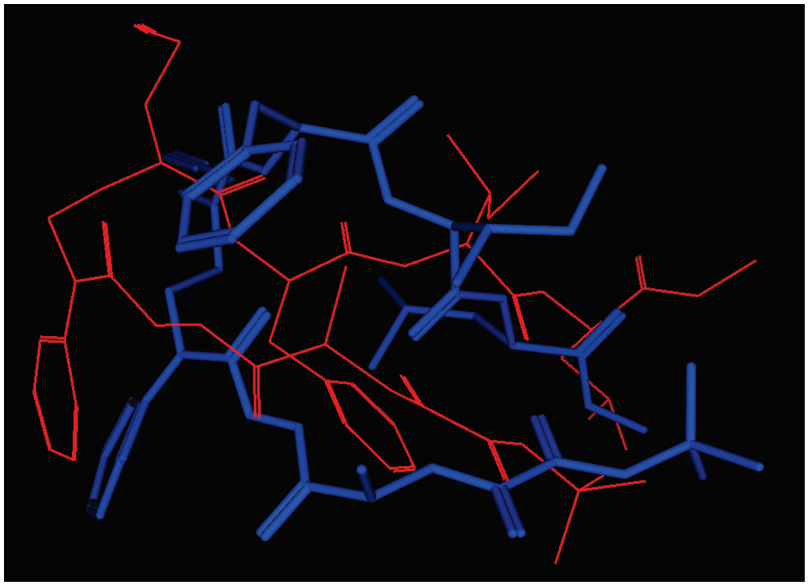

FIGURE 6. 13, Backbone-rmsd superposition of the two single most abundantly sampled motifs of the 100 ns MD runs at 290 K. Blue stick and red line renderings represent $CDCl_3$ ($\varepsilon = 4.8$) and MeOH ($\varepsilon = 32.5$) trajectories, respectively. Hydrogens omitted for clarity.

interactions. To obtain tight interactions, backbone-modifying peptidomimetic scaffolds must aim at reproducing the spatial arrangements adopted by the lining functionalities as closely as possible while at the same time maintaining straightforward synthetic diversification. Then, for our purposes, we require strand-extended ensembles of folds with the strands in parallel alignment before and after the turn, sampling a satisfactorily small rmsd section of conformational space. In general, foldability is thought of as an enthalpic gain that must be realized via weak interactions, eventually overcompensating the entropic penalty for intrastrand ordering.[32] β-sheets in proteins are characteristically stabilized by cross-strand hydrogen bonds; this may be favorably so because they preferentially occur in a hydrophobic pocket of the protein where the solvent cannot effectively compete in the donor−acceptor interaction.[27a] On the contrary, a small oligomer peptidomimetic like **13** will likely always experience full solvent exposure. In a competing environment such as a polar solvent, the resulting reversibility of association and thus kinetic lability of folds[33] are decisive impediments toward successful hydrogen bonding directed self-assembly without relying on any support provided by additional conformation-fixing strand increments (templates), covalent cross-linking, and the like.

NMR studies of NXO-based β-mimics verify the presence of substantial amounts of folded conformers in solution. Pertinent cross-strand NOEs in the mimics resemble those in the closest analogues known in the literature and are well-reproduced by molecular dynamics simulations in implicit solvent. Strongly (*ap*) constrained "N" hydrazide and "O" oxalamide backbone dihedrals rigidify the potential energy surface in the extended N^{L}AlaO-tripeptide, which, in turn, restrains the "X" amino acid orientation in the octapeptide β-sheet mimic **13** to characteristic Φ, Ψ values. When **13** is subjected to a competitive solvent, the turn linker gives way and thus ensemble homogeneity is decreased. Still, the core conformer populates the same rmsd space. These studies of an NXO-modified β-mimic encourage further endeavors toward NXO-peptidomimetics that fold to predictable secondary structure in aqueous solution.[34]

Experimental Section

Preparation of Orthogonally Protected NXO Building Blocks 3. General Procedure. The mixture of amino acid **1** and alkyl-4-nitrophenyloxalate (1.1 equiv) **2** in dry DMF was stirred at 50 °C until the solution had become clear (1.5−2.0 h). The reaction mixture was allowed to cool to room temperature. Subsequently, HOBt (1.05 equiv), DCC (1.05 equiv), and the corresponding protected hydrazine (1.0 equiv) were added and the mixture was stirred at room temperature under argon for 5 h. DMF was evaporated under reduced pressure on a rotary evaporator; the residue obtained was dissolved in ethyl acetate and precipitated dicyclohexyl urea was removed by filtration. The ethyl acetate solution was washed with 1 N HCl and 10% $NaHCO_3$ followed by brine and dried over Na_2SO_4. After evaporation of solvent, the crude compound was purified by flash column chromatography to give the required compound **3** as a solid.

Preparation of Pseudopeptides 4. Trifluoroacetic acid (TFA, 1.5 equiv) was added slowly with stirring at 0 °C to a solution of **3** in CH_2Cl_2. The reaction mixture was stirred under argon at room temperature for an additional 30 min. Solvent was evaporated and the crude residue was dried well under high vacuum. The material obtained was dissolved in CH_2Cl_2 and neutralized by triethylamine (TEA) (2 equiv). In another flask, Boc-L-amino acid (1 equiv), EDCI·HCl (1 equiv), and HOBt (1 equiv) were dissolved in CH_2Cl_2. TEA (1 equiv) was added to this mixture and the reaction mixture was stirred for 15 min at room temperature under argon. Then, the first prepared solution was added to this mixture and stirred overnight at room temperature. The solvent was removed by rotary evaporation

(32) Jager, M.; Deechongkit, S.; Koepf, E. K.; Nguyen,J.; Gao, J.; Powers, E. T.; Gruebele, M.; Kelly, J. W. *J. Pept. Sci.* **2008**, *90*, 751−758 and references cited therein; see also refs 8b and 27b.

(33) Baldwin, R. L. *J. Biol. Chem.* **2003**, *278*, 17581–17588.

(34) NXO building blocks are offered by *Senn* Chemicals AG, CH-8157 Dielsdorf, www.sennchem.com, who have obtained an exclusive license from the Vienna University of Technology.

and the residue obtained was dissolved in ethyl acetate. The ethyl acetate solution was washed with 1 N HCl, 10% $NaHCO_3$, and brine, dried (Na_2SO_4), and concentrated to give **6** as a colorless solid.

A solution of LiOH (12 equiv) in a minimum amount of water was added dropwise to a solution of **6** in MeOH. The reaction mixture was further stirred for 1 h. MeOH was then evaporated and the residue obtained was dissolved in water, washed with ether, acidified with 1 N HCl, and extracted with ethyl acetate. The combined ethyl acetate layers were washed with brine, dried (Na_2SO_4), and concentrated. The crude compound was triturated with diethyl ether and filtered to give **7** as a colorless solid.

HOBt (1.05 equiv) and EDCI·HCl (1.05 equiv) were added to a solution of **7** in CH_2Cl_2; the mixture was stirred for an additional 15 min. A solution of L-amino acid dimethylamide (1.05 equiv) in CH_2Cl_2 was added followed by TEA (1.05 equiv) then the mixture was stirred overnight at room temperature. The solvent was removed by rotary evaporation and the residue obtained was dissolved in ethyl acetate, washed with 1 N HCl, 10% $NaHCO_3$, and brine, dried (Na_2SO_4), and concentrated to give crude product, which was recrystallized from ethyl acetate to give **4** as a colorless solid.

Preparation of NXO β-Sheet Mimic 13. Preparation of compound 16: (*S*)-(4-{*N*′-[2-(*tert*-Butylaminooxalylamino)propionyl]hydrazino}-4-oxo-3-phenylbutyl)carbamic Acid 9*H*-Fluoren-9-ylmethyl Ester. To a solution of compound **15** (900 mg, 1.7 mmol) in CH_2Cl_2 (10 mL) was added TFA (10 mL) slowly with stirring at 0 °C; the reaction mixture was further stirred under argon at room temperature for 30 min (after overnight stirring there is formation of byproduct so stirring only for 30 min is crucial). Solvent was evaporated and the residue was dried well under high vacuum and dissolved in CH_2Cl_2 (15 mL). In another flask, compound **18** (377 mg, 1.74 mmol, prepared in three steps and 67% overall yield from L-alanine methyl ester hydrochloride, see the Supporting Information), HOBt (247 mg, 1.83 mmol), and DCC (377 mg, 1.83 mmol) were dissolved in CH_2Cl_2 (15 mL) and the mixture was stirred for 15 min at room temperature; hereto, a mixture of the above TFA salt of **15** and DIPEA (0.34 mL, 1.92 mmol) in CH_2Cl_2 (15 mL) were added and the mixture was stirred overnight at room temperature. The precipitated dicyclohexyl urea (DCHU) was removed by filtration and the filtrate was evaporated. Remaining DCHU was removed by subsequent trituration with cold ethyl acetate and filtration. The ethyl acetate solution was washed with 1 N HCl (15 mL), 10% $NaHCO_3$ (15 mL), and brine (15 mL), dried (Na_2SO_4), and concentrated to give 1.1 g of crude compound, which was purified by column chromatography to give 974 mg (90%) of product as a white solid; mp 48−49 °C.

Preparation of compound 17: (*S*)-*N*-*tert*-Butyl-*N*′-(1-{*N*′-[4-(2-cyanoethylamino)-2-phenylbutyryl]hydrazinocarbonyl}ethyl)-oxalamide. A solution of compound **16** (915 mg, 1.49 mmol) in 10% piperidine in CH_2Cl_2 (15 mL) was stirred at room temperature for 20 min. Solvent was evaporated and the reaction mixture was dried well under high vacuum to remove the last traces of piperidine. The residue thus obtained was crystallized from ethyl acetate−pentane to give 575 mg (98%) of free amine. The free amine was dissolved in methanol (15 mL); hereto was added acrylonitrile (0.15 mL, 2.23 mmol) and the reaction mixture was stirred overnight at room temperature under argon. The solvent was evaporated and the crude compound was purified by column chromatography to give 333 mg (50%) of product as a white solid; mp 62−63 °C.

Preparation of Compound 13. (*all-S*)-*N*-*tert*-Butyl-*N*′-(1-{*N*′-[4-(1-(2-cyanoethyl)-3-{1-[2-methyl-1-(3-methyl-1-methylcarbamoylbutylcarbamoyl)butylcarbamoyl]-2-phenylethyl}ureido)-2-phenylbutyryl]hydrazinocarbonyl}ethyl)oxalamide. The NH-BOC derivative **24** (363 mg, 0.82 mmol) was deprotected with 5 mL of satd HCl in ethyl acetate at 0 °C for 60 min under Ar atmosphere followed by evaporation, overnight drying. To this crude HCl-salt were added 10 mL of CH_2Cl_2 and 10 mL of saturated aqueous $NaHCO_3$ and the biphasic mixture was cooled to 0 °C in an ice bath. Stirring was stopped, the layers were allowed to separate, and a 1.93 M solution of phosgene in toluene (0.85 mL, 1.64 mmol) was added in a single portion via syringe to the lower (organic) phase. Stirring was resumed immediately, and the ice-cooled reaction mixture was stirred vigorously for 10 min at 600 rpm. The layers were then allowed to separate, the aqueous phase was extracted with CH_2Cl_2 (3 × 5 mL), and the combined organic layers were dried over Na_2SO_4, filtered, and concentrated by rotary evaporation. The obtained residue was dissolved in toluene (15 mL); hereto was added **17** (333 mg, 0.75 mmol). The reaction mixture was further refluxed overnight, evaporated to dryness, diluted with ethyl acetate, washed with 10% aq $NaHCO_3$ and brine, dried over Na_2SO_4, and evaporated to give crude compound, which was purified by column chromatography to give (68%) the desired compound as a white solid; mp 144−145 °C.

Computational Methods. Calculations were performed with use of th eMolecular Operating Environment, Version 2007.09 (MOE, 1997−2007, Chemical Computing Group Inc.). Input geometries were obtained from stochastic conformational searching employing the OPLS-AA force field potential parameters and performed with soft distance constraints derived from qualitatively assigned experimental NOE intensities. The lowest energy conformers thus obtained were freed of all restraints and subjected to molecular dynamics simulations in an NVT ensemble. Solvents as in the NMR experiment were treated implicitly by the generalized Born solvation model setting the exterior dielectric to the value of $\varepsilon = 4.8$ or 32 D for $CDCl_3$ and d_3-MeOH, respectively.

Acknowledgment. We thank Senn Chemicals AG for financial support. Our gratitude to Prof. Oliver Zerbe and Nadja Bross from the Institute of Organic Chemistry, University of Zurich, for the measurement of NMR spectra. J.P. thanks the ÖAD-Österreichischer Austauschdienst (Austrian Exchange Service) for a doctoral grant. The project was funded in part by the uni:invent PRIZE grant (Z060414) of the Austria Wirtschaftsservice G.m.b.H. (aws).

Supporting Information Available: Experimental procedures, characterization data for all new compounds, and spectral and computational data. This material is available free of charge via the Internet at http://pubs.acs.org.